Advances in Geo-Energy Research

Vol. 16, No. 3, p. 244-259, 2025

Original article

Multi-fidelity machine learning with knowledge transfer enhances geothermal energy system design and optimization

Guodong Chen[1,2], Jiu Jimmy Jiao[1]*, Zhongzheng Wang[3], Qinyang Dai[4]

[1]*Department of Earth Sciences, The University of Hong Kong, Hong Kong 000000, P. R. China*

[2]*Robert Frederick Smith School of Chemical and Biomolecular Engineering, Cornell University, Ithaca 14850, USA*

[3]*College of Engineering, Peking University, Beijing 100871, P. R. China*

[4]*School of Petroleum Engineering, China University of Petroleum (East China), Qingdao 266580, P. R. China*

Keywords:
Knowledge transfer
machine learning
enhanced geothermal system
heat extraction optimization
data-driven optimization

Cited as:
Chen, G., Jiao, J. J., Wang, Z., Dai, Q. Multi-fidelity machine learning with knowledge transfer enhances geothermal energy system design and optimization. Advances in Geo-Energy Research, 2025, 16(3): 244-259.
https://doi.org/10.46690/ager.2025.06.05

Abstract:
Designing and optimizing the control schemes of geothermal energy systems is a challenging and time-consuming work due to the vast parameter space and computationally intensive simulations. Canonical evolutionary optimization approaches are laborious, slow to converge, and may not provide optimal well-control scheme for geothermal energy systems. To tackle these issues, this work reports a machine learning-guided real-time flow control optimization for enhanced geothermal systems. This approach fully leverages existing data throughout the optimization phase by creating multi-fidelity surrogate models, which comprise coarse and fine models. The coarse model strategically selects a subset of variables to develop a low-fidelity representation, while the fine model utilizes all available variables to construct a high-fidelity surrogate. Knowledge transfer from coarse surrogate can guide the fine surrogate search into a promising subspace. Active learning technique is further leveraged to improve the accuracy of surrogate by iteratively querying the most informative data points. To evaluate effectiveness of the proposed approach, benchmark function suites and two fractured geothermal energy systems are employed in comparison with conventional evolutionary algorithms and advanced surrogate-assisted methods. The results illustrate the capability of the workflow to enhance the efficiency and effectiveness of real-time decision making. This workflow paves a new path for complex and computationally intensive design optimization problems.

1. Introduction

Enhanced Geothermal Systems (EGS) are considered as a promising source to attain enduring and sustainable energy for the purpose of electricity generation (Menberg et al., 2016; Jolie et al., 2021). Heat extraction of geothermal energy from fractured geothermal systems is challenging because the fractures may cause low sweep efficiency and early breakthrough of the injected cold water. The advancement of geothermal energy development has faced severe challenges from both technical and economic standpoints (Menberg et al., 2016; Parisio et al., 2019). Numerous geothermal reservoirs have been forsaken due to their low heat output and the associated risks stemming from subsurface intricacies along with uncertainties. Moreover, numerous EGS projects are not viable from a commercial standpoint due to challenges like thermal breakthrough, as well as fluid loss during the exploitation process. Advanced numerical simulations that utilize methods such as the finite element method have been extensively applied to describe subsurface fluid flow and heat transfer behaviors in geothermal energy systems (Li et al., 2019). Numerical simulations serve to delineate the intricate interplay between

Yandy Scientific Press

*Corresponding author.
E-mail address: gc594@cornell.edu (G. Chen); jjiao@hku.hk (J. J. Jiao); wangzzgr@163.com (Z. Wang); dai_qinyang@163.com (Q. Dai).

Received March 21, 2025; revised April 17, 2025; accepted May 5, 2025; available online May 9, 2025.

subterranean fluids and rock formations, thereby enabling the prognostication of geothermal energy distributions. Mathematical methods commonly employed for fractured porous media encompass the equivalent porous media method (Hsieh et al., 1985), dual-porosity method (Zimmerman et al., 1993), and discrete fracture network method (Li et al., 2019). Continuum method treats fractures as a heterogeneous porous medium, while discrete fracture network model explicitly characterizes the fractures, thus enabling a more realistic simulation of fluid flow and heat transport (Hyman et al., 2019).

For geothermal energy production, accurate estimation of subsurface fracture network distribution via inverse modelling is a prerequisite to make further decision making (Chen et al., 2023). Common geological monitoring methods for detecting fracture distribution include are terrestrial laser scanning (Pan et al., 2019), fractured core analysis (Ghanizadeh et al., 2016) and seismic wave analysis (Xu et al., 2022; Jiang et al., 2023). After reliable characterization of fracture networks, the optimal development of the geothermal energy system can be determined via optimization theory. Optimal development and management of geothermal energy systems play a key role in increasing the reservoir recovery of geothermal energy. Such complex real-world optimization problems are conspicuous across a multifarious array of disciplines, spanning the scientific, engineering, and industrial domains (Ding et al., 2021; Li et al., 2023a). Evolutionary algorithms including Differential Evolution (DE) (Xue et al., 2022) have successfully spread widely due to the promising global search capabilities and simplicity of structure (Eiben and Smith, 2015; Zhang et al., 2021b). In the absence of extensive prior knowledge and the soaring dimensions of variables of the complex system, the parameter space rises exponentially for the optimal design (Song et al., 2022). In particular, each calculation of objective function requires computationally intensive hydrothermal simulation, rendering an exhaustive search with evolutionary algorithm impractical, if not unattainable.

Machine Learning (ML) has gained intensive research and substantially advanced renewable and sustainable energy development and a series of other scientific and industrial problems in recent years (Sanchez-Lengeling and Aspuru-Guzik, 2018; Sun et al., 2023; Chen et al., 2024b; Wang et al., 2025). ML approximates the underlying mapping between the input and the target function values in multidimensional parameter space to replace the real calculation of high-fidelity simulations (Xue et al., 2021; Wang et al., 2023). Many data-driven optimization methods use ML models as surrogates, including artificial neural networks, Gaussian processes (Fan et al., 2019), support vector machines (Zhang et al., 2021a), and Radial Basis Function (RBF) networks (Chen et al., 2022), to guide the search of evolutionary algorithms. Data-driven optimization can be divided into two types: offline surrogates, which build ML models using one-time samples, and online surrogates, which build models based on Design of Experiment (DoE) while continuously incorporating informative samples(Li et al., 2023b). Past studies have utilized multivariate adaptive regression splines as offline surrogates to examine the effects of geological uncertainties on optimal well placement and control (Chen et al., 2015). Asai et al. (2018) trained a polynomial surface regression function to explore the sensitivity of key variables in geothermal systems. Wang et al. (2022) used random forest as a surrogate and combined genetic algorithm to determine the optimal geothermal well placement in heterogeneous geothermal reservoirs. Yan et al. (2023) combined a feed-forward neural network and non-dominated sorting-based genetic algorithm II taking uncertainties of rock properties into consideration to achieve robust optimization. However, most existing optimization algorithms for geothermal energy extraction mainly use offline surrogate without further infilling of samples, resulting in relatively low prediction accuracy and high uncertainty of the final provided optimal solution.

Online surrogate-assisted optimization has garnered significant attention for its remarkable efficacy in addressing intricate and resource-intensive problems within limited computational budget (Zhang et al., 2022; Du et al., 2023). This approach employs an active learning framework that interacts with fractured hydrothermal simulations to enhance the surrogate iteratively (Jin et al., 2018). New samples are queried sequentially to uncover the optimized decision variables. Yu et al. (2018) have proposed a surrogate-based hierarchical particle swarm optimization to collaboratively explore and exploit the design space using two optimizers. Deng et al. (2022) introduced a self-directed online learning for topology optimization, where finite element simulation is replaced by a deep neural network and training samples are generated dynamically using the prediction of the optimum of the surrogate. Despite the significant strides made in online data-driven optimization, the performance of these algorithms deteriorates dramatically when solving multi-dimensional resource-intensive optimization challenges.

In the realm of geothermal energy system design and optimization, two main challenges are encountered (Chen et al., 2024a): how to construct an ML model with limited historical data to assist further decision-making efficiently and effectively; how to iteratively infill the most informative samples to enhance the accuracy of surrogates and accelerate convergence. This study endeavors to surmount these challenges through the knowledge transfer between multi-fidelity ML surrogates to enhance geothermal energy systems design. The contributions of this research are summarized as:

1) In order to harness the full breadth of data and knowledge within the optimization process, multi-fidelity surrogates, specifically coarse and fine models, are developed. The coarse model selects part variables to construct a low-fidelity model with GRNN, while the fine surrogate uses all variables to construct a high-fidelity model with RBF network. The coarse surrogate focuses on capturing the global trends of the objective function's landscape, whereas the fine surrogate aims to explore promising subregions. The synergy of these multi-surrogate models is expected to mitigate local optimums and ensure the identification of global optimum solutions.
2) A divide-and-conquer optimization paradigm is devised, wherein the large multidimensional problem is divided into two groups. A coarse surrogate is established to

capture trends in the fitness landscape. Knowledge transfer from the coarse model to the fine model is then implemented to guide the fine model search, enhancing the exploitation of promising areas with greater accuracy.

3) Active learning techniques are utilized to improve the precision of surrogates by iteratively querying the most informative solutions within the parameter space. Considering that relying solely on an offline surrogate without further infilling samples may result in relatively low accuracy of prediction and high uncertainty of the final provided optimal solution, active learning is employed to refine the ML model and iteratively select the most informative samples based on informed acquisition function. This strategy allows for more accurate ML predictions and fewer simulation evaluations, enabling faster convergence by orders of magnitude.

This study presents a novel demonstration of online optimization for geothermal energy systems through knowledge transfer across multi-fidelity ML. The proposed method significantly reduces computational time for designing and optimizing geothermal energy systems compared to traditional heuristic methods and surrogate-guided methods. This advancement holds great promise for addressing complex, computationally intensive and practical challenges, spanning from CO_2 sequestration (Wen et al., 2023), smart grid management (Yao et al., 2023), to mechanical metamaterials design (Bastek and Kochmann, 2023).

2. Methods

2.1 Hydrothermal coupling and governing equations

2.1.1 Mass balance equation

The conservation of mass in subsurface groundwater flow, pertinent to porous and discrete fracture network media constituting geothermal reservoirs, can be meticulously articulated through the mass balance equation as:

$$\frac{\partial}{\partial t}(\rho_f \phi) + \nabla(\rho_f u) = \Psi_{mf} + Q_m \tag{1}$$

where t denotes time variable, ρ_f indicates fluid density, ϕ signifies porosity, Ψ_{mf} represents the flux transfer function linking fractures with porous media, Q_m indicates the mass source term, and u characterizes fluid velocity, which is mathematically defined as follows:

$$u = -\frac{k}{\mu}(\nabla p + \rho_f g \nabla D) \tag{2}$$

where k is permeability (the permeability the permeability associated with fractures adheres to the cubic law $k_f = b^2/12$, b represents the fracture aperture), μ signifies the viscosity, p stands for pressure, g indicates gravitational acceleration, and ∇D is the unit directional vector aligned with the gravitational force. The flux transfer function Ψ_{mf} is given by:

$$\Psi_{mf} = \nabla\left(-\rho_f \frac{k}{\mu}\nabla P_b\right) \tag{3}$$

where ∇P_b represents the pressure gradient within the fracture tangent direction.

2.1.2 Energy balance equation

The energy balance equation governs both advective and conductive heat transfer in a porous medium:

$$(\rho_f C)_{eff}\frac{\partial T}{\partial t} + \rho_f C_w u_m \nabla T - \nabla(\lambda_{eff}\nabla T) = E_{mf} + Q_{hm} \tag{4}$$

where C represents specific heat capacity, $(\rho C)_{eff} = \phi\rho_f C_w + (1-\phi)\rho_s C_s$ represents the effective heat capacity, λ refers to thermal conductivity, $\lambda_{eff} = \phi\lambda_w + (1-\phi)\rho_s C_s$ describes the effective thermal conductivity, s and w indicate the subsurface solid and water, $E_{mf} = h(T_f - T_m)$ represents the heat transport within fractures and matrix, h represents convective thermal transport coefficient within matrix and fractures, and Q_{hm} denotes heat source/sink term in porous media. Heat transfer within fractures of EGS is given by:

$$b\rho_f C_f \frac{\partial T}{\partial t} + b\rho_f u_f C_f \nabla_T T - \nabla_T(b\lambda_f \nabla_T T) = E_{fm} + Q_{hf} \tag{5}$$

where $E_{fm} = h(T_m - T_f)$ represents the heat transport within matrix and fractures, and Q_{hf} represents the heat source/sink term in fractures.

2.2 Related optimization techniques

2.2.1 Generalized regression neural network

As initially introduced by Specht (1991), Generalized Regression Neural Network (GRNN) is a memory-based neural network adept at estimating the underlying regression surface. Notably diverging from the feed-forward neural network paradigm, GRNN engenders the model in a one-pass learning mode devoid of iterative tuning. The computationally efficient property of GRNN makes it suitable for solving expensive optimization problems. The architecture of GRNN includes input layer, pattern layer, summation layer, and output layer. The conditional mean of the output is expressed as:

$$E[y|\mathbf{x}] = \frac{\int_{-\infty}^{\infty} y f(\mathbf{x},y)\mathrm{d}y}{\int_{-\infty}^{\infty} f(\mathbf{x},y)\mathrm{d}y} \tag{6}$$

where $f(\mathbf{x},y)$ is the joint probability density function for input $\mathbf{x}$. With given data $\{(\mathbf{x}_i,y_i)|\mathbf{x}_i \in \mathrm{R}^d\}$, this joint probability density function is calculated as:

$$\hat{f}(\mathbf{x},y) = \frac{1}{N(2\pi)^{(D+1)/2}\sigma^{D+1}}\sum_{i=1}^{N}\exp\left[-\frac{(\mathbf{x}-\mathbf{x}_i)(\mathbf{x}-\mathbf{x}_i)^T}{2\sigma^2}\right]\exp\left[-\frac{(y-y_i)^2}{2\sigma^2}\right] \tag{7}$$

where σ is the shape parameter. Thus, the output function value can be calculated as:

$$E(y|\mathbf{x}) = \frac{\sum_{i=1}^{N} y_i \exp\left[-\frac{(\mathbf{x}-\mathbf{x}_i)(\mathbf{x}-\mathbf{x}_i)^T}{2\sigma^2}\right]}{\sum_{i=1}^{N}\exp\left[-\frac{(\mathbf{x}-\mathbf{x}_i)(\mathbf{x}-\mathbf{x}_i)^T}{2\sigma^2}\right]} \tag{8}$$

2.2.2 RBF network

RBF has gained considerable acclaim in the realm of scientific and engineering domains owing to its remarkable capacity to approximate the intricacies of the objective function landscape, even when armed with a limited number of sample points. Its resilience to high dimensionality and effectiveness in addressing complex problems make RBF an ideal choice for this study. RBF serves as an approximation model characterized by a weighted sum of kernel functions:

$$\hat{f}(\mathbf{x}) = \sum_{i=1}^{N} \omega_i \varphi(\|\mathbf{x} - \mathbf{c}_i\|) \tag{9}$$

where ω denotes the weight coefficient, $\varphi(\cdot)$ is kernel function, $\|\cdot\|$ represents Euclidean distance, and $\mathbf{c}_i$ indicates the i^{th} center sample point. For given training set $\{(\mathbf{x}_1, y_1), \ldots, (\mathbf{x}_N, y_N)\}$, the weight coefficient can be given by:

$$\boldsymbol{\omega} = \boldsymbol{\Psi}^{-1}\mathbf{y} \tag{10}$$

with $\boldsymbol{\Psi} = [\varphi(\|\mathbf{x}_i - \mathbf{x}_j\|)]_{N\times N}$ the kernel matrix. To accelerate the training and avoid the overfit risks, the shape parameters σ^2 is empirically set as $dis_{\max}(dn)^{-1/d}$, with $dis_{\max}$ the maximum distance between samples.

2.2.3 DE

DE is a robust metaheuristic algorithm well-suited for complex optimization problems due to its global search capabilities and structural simplicity. The algorithm uses a population - based approach to maintain a set of candidate individuals that evolve over generations through the application of evolutionary operators such as mutation and crossover. The initial population $\mathbf{P} = [\mathbf{x}_1, \ldots, \mathbf{x}_i, \ldots, \mathbf{x}_{NP}], i = \{1, \ldots, NP\}, \mathbf{x}_i \in \mathbb{R}^d$ is randomly sampled from the parameter space $[\mathbf{lb}, \mathbf{ub}]$, by the lower and upper bounds **lb**, **ub**. Classical DE employs three main steps: mutation, crossover, and selection. The mutant vectors $[\mathbf{v}_1, \ldots, \mathbf{v}_i, \ldots, \mathbf{v}_{NP}], i = \{1, \ldots, NP\}, \mathbf{x}_i \in \mathbb{R}^d$ are generated with the mutation operator:

$$\mathbf{v}_i = \mathbf{x}_{best} + Mu \times (\mathbf{x}_{r_1} - \mathbf{x}_{r_2}) \tag{11}$$

where r_1 and r_2 indicate sampled integers between 1 and NP obeying uniform distribution, Mu indicates mutation factor, and $\mathbf{x}_{best}$ represents the best individual within population. Crossover operator then produces trial vectors via:

$$\mathbf{u}_i^j = \begin{cases} \mathbf{v}_i^j & \text{if rand} \le CR \text{ or } j = j_{\text{rand}} \\ \mathbf{x}_i^j & \text{otherwise} \end{cases}, j \in \{1, \ldots, d\} \tag{12}$$

where $\mathbf{u}_i^j$ denotes the j^{th} parameter for the i^{th} trial vector, *rand* represents a sampled number between 0 and 1 obeying uniform distribution, and CR indicates the crossover factor. The fitness value of trial vector **u** is calculated and offspring is produced via:

$$\mathbf{x}_i' = \begin{cases} \mathbf{u}_i & if\ f(\mathbf{u}_i) < f(\mathbf{x}_i) \\ \mathbf{x}_i & otherwise \end{cases} \tag{13}$$

where $\mathbf{x}_i'$ is the i^{th} new individual of the next population.

2.2.4 Knowledge transfer in optimization

Knowledge transfer holds the potential to enrich problem-solving capabilities, particularly within the realm of evolutionary optimization (Jin, 2013; Wang et al., 2021). The acquisition of knowledge garnered from the optimization process, coupled with its judicious integration into evolutionary algorithms, has demonstrably proven to be instrumental in hastening convergence and elevating the quality of derived optimal solutions (Yang et al., 2019). Notably, the utilization of knowledge transfer draws upon optimal solutions derived from analogous antecedent problems, repurposing them as shared knowledge and integrating them into the initial population to address the current challenge (Gupta et al., 2017; Liu et al., 2023). Moreover, scholarly inquiries delving into the reappropriation of knowledge from disparate problems have been on the rise (Xue et al., 2020), with methodologies now poised to efficiently transpose structured knowledge gleaned from preceding tasks onto the present undertaking.

Multifactorial evolutionary algorithms (Gupta et al., 2015; Xue et al., 2021) have surfaced as a conduit for knowledge transfer among parallel tasks, engendering knowledge exchange through the conduits of assortative mating and vertical cultural transmission. These techniques enable the individual tasks to not only preserve their unique knowledge but also acquire knowledge from other tasks, fostering a more comprehensive and enriched problem-solving approach. Motivated by the achievements of knowledge transfer in evolutionary computation, this work proposes the utilization of knowledge transfer techniques to enhance the capability of surrogates in expediting optimization. High-fidelity and low-fidelity surrogates are constructed with historical samples and shared knowledge during the optimization search. The optimization performance can be further enhanced by multi-fidelity ML models with knowledge transfer, bearing substantial significance for complex optimization entwined with computationally intensive simulations.

3. Knowledge transfer between multi-fidelity ML

3.1 Problem formulation

Geothermal energy system encompasses both above-ground and subsurface infrastructure, designed to enable the extraction of heated fluid for either generating power or heating purposes. A thorough economic analysis is crucial for the comprehensive investigation of an EGS, closely linked to the results of forward hydrothermal simulations. The main goal of optimizing heat extraction is to maximize the Net Present Value (NPV) of the geothermal reservoir throughout the exploitation duration. With water serving as the working fluid, the profitability associated with developing the geothermal reservoir can be represented in terms of the net value derived from energy production, which considers the costs related to both water extraction and reinjection. Consequently, the design and optimization problems of geothermal energy systems can be mathematically represented as:

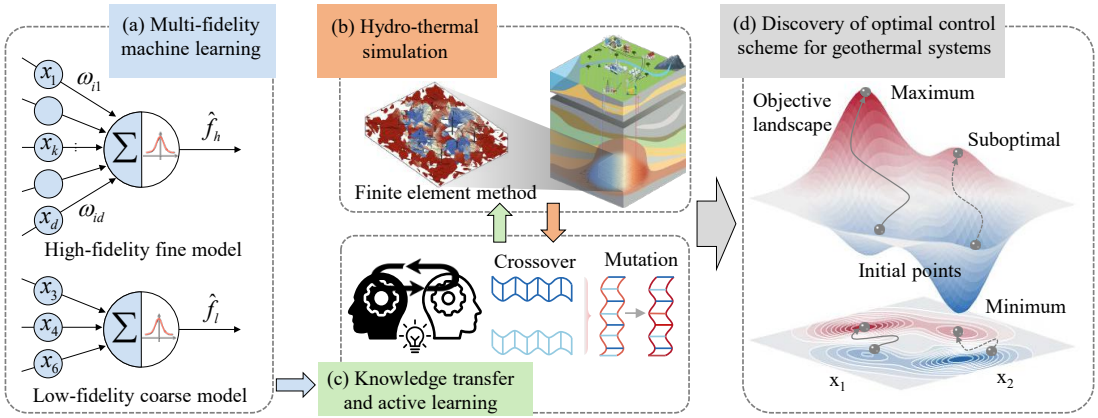

Fig. 1. Overview of the proposed workflow. (a) Multi-fidelity coarse and fine ML models, (b) hydro-thermal numerical simulation based on finite element method, (c) knowledge transfer between multi-fidelity surrogates and active learning to query new samples and (d) discovery of optimal control schemes for EGS.

Algorithm 1: Pseudo code of MFSKT.

Input : Database D, population NP, number of training samples τ, mutation factor Mu, crossover factor CR, maximum limit of simulation evaluations $FES_{\max}$

Output: The optimal sample $\mathbf{x}_{best}$ and database D

Sample τ initial solutions using LHS;
Calculate the objective values of the samples using simulator;
$FES = \tau$;
while $FES < FES_{\max}$ **do**
  Determine the coefficient $r = \text{rand}([0,1])$;
  Calculate the dimension of coarse model d_i;
  Select d_i variables with index $\{r_1, \ldots, r_{d_i}\}$ from the original d variables;
  Obtain $\hat{\mathbf{u}}_{s_{best}}$ by conducting coarse surrogate pre - screening; ; `// Algorithm 2`
  Transfer knowledge from coarse model to fine model by injecting $\hat{\mathbf{u}}_{s_{best}}$;
  Conduct fine surrogate search; ; `// Algorithm 3`
  Generate final candidate solution $\hat{\mathbf{x}}_{can}$;
  Calculate the objective value of $\hat{\mathbf{x}}_{can}$ using hydro - thermal simulation;
  $FES = FES + 1$;
  Add the infilled solution and associated fitness value to database D;
  Update the current found optimal sample $\mathbf{x}_{best}$;
end
return

$$\begin{aligned} &\max \text{NPV}(\mathbf{x}, \mathbf{z}), \mathbf{x} \in \mathbb{R}^d \\ &\text{s.t. } \mathbf{lb} \le \mathbf{x} \le \mathbf{ub} \\ &c(\mathbf{x}) \le 0 \end{aligned} \tag{14}$$

where **lb** and **ub** represent lower and upper boundaries of the parameters to be optimized respectively, and c represents the physical or operational constraints of the parameters to be optimized. NPV is given by:

$$\text{NPV}(\mathbf{x}, \mathbf{z}) = \text{CTEP} \times r_e - \text{CWI} \times r_i - \text{CWP} \times r_p \tag{15}$$

where $\mathbf{x}$ represents the parameters to be determined, $\mathbf{z}$ describes the state parameters such as temperature and pressure, CTEP, CWI, and CWP represent the cumulative thermal energy production, fluid injection, and fluid production, r_e, r_i and r_p are the price of thermal energy, the cost of fluid injection and fluid production, respectively.

3.2 General framework of the proposed method

A Multi-fidelity Surrogate with Knowledge Transfer (MFSKT) is proposed for expensive optimization design problems, typically geothermal systems design. Overview of the developed workflow is delineated in Fig. 1. Deep learning holds powerful learning ability in predicting fluid flow and heat transfer dynamics. However, these methods require a large amount of training samples, making it computationally prohibitive for such large-scale time-consuming simulation models. When only limited simulation evaluations are available, GRNN and RBF ML methods work well for such small sample problems. The algorithm begins with DoE using Latin Hypercubic Sampling (LHS), followed by the construction of multi-fidelity ML models. Knowledge transfer from low-fidelity surrogate to high-fidelity surrogate can guide the search into a promising subspace, thus augmenting the search capability. Active learning is harnessed to further improve the accuracy of the ML model through the iterative infusion of the most informative samples within parameter space.

For one iterative loop, a coarse low-fidelity surrogate using GRNN is constructed with a portion of randomly selected parameters in a subspace, followed by the preselection of the most promising individual from the candidate offspring by the coarse surrogate. Subsequently, Knowledge transfer with the selected individual is conducted from the coarse model to the fine model. Evolutionary search is then conducted for the remaining parameters with the assistance of fine surrogate. The most promising solution is selected for simulation evaluations. The detailed pseudo code of multi-fidelity surrogates with knowledge transfer is elucidated in Algorithm 1.

Algorithm 2: Pseudo-code of coarse surrogate pre-screening.

Input : Database D, population NP, number of training samples τ, index $\{r_1,\ldots,r_{d_i}\}$ of d_i variables, mutation factor Mu, crossover factor CR, the maximum limit of simulations $FES_{\max}$

Output: The candidate solution $\hat{\mathbf{u}}_{s_{best}}$ to be transferred

Reduce the database D to sub-database D_s by extracting d_i variables with index $\{r_1,\ldots,r_{d_i}\}$;
Choose τ best samples as training samples from sub-database D_s;
Construct coarse surrogate $\hat{f}_{coa}$ using GRNN;
Select NP best sample points $P=\{\mathbf{x}_{s_1},\ldots,\mathbf{x}_{s_i},\ldots,\mathbf{x}_{s_{NP}}\}$ from sub-database D_s;
Generate offspring $P'=\{\mathbf{u}_{s_1},\ldots,\mathbf{u}_{s_i},\ldots,\mathbf{u}_{s_{NP}}\}$ using differential evolutionary operator;
Pre-screen the most promising individual $\hat{\mathbf{u}}_{s_{best}}$ by coarse surrogate $\hat{f}_{coa}$;

Algorithm 3: Pseudo code of fine surrogate search.

Input : Database D, number of training samples τ, mutation factor Mu, crossover factor CR, the Upper limit of generations $Gens_{\max}$, the candidate solution $\hat{\mathbf{u}}_{s_{best}}$ to be transferred

Output: The best solution $\hat{\mathbf{x}}_{can}$

Choose τ best samples as training samples from database D;
Construct fine surrogate $\hat{f}_{fine}$ using RBF network;
Select NP best samples $P=\{\mathbf{x}_1,\ldots,\mathbf{x}_i,\ldots,\mathbf{x}_{NP}\}$ from database D as current population;
for $Iters=1:Gens_{\max}$ **do**
    Conduct evolutionary operator (mutation and crossover) to generate new offsprings;
    Transfer knowledge $\hat{\mathbf{u}}_{s_{best}}$ from low-fidelity surrogate to offsprings;
    Evaluate the fitness value of current offsprings with fine surrogate $\hat{f}_{fine}$;
    Update the population P according to the predicted fitness value;
end
Select the most promising individual $\hat{\mathbf{x}}_{can}$ by fine surrogate $\hat{f}_{fine}$;

3.3 Coarse surrogate pre-screening

According to the "divide-and-conquer" paradigm, the large optimization problem is randomly divided into two groups controlled by coefficient r:

$$d_l = r \times d \tag{16}$$

where d is the dimension of problem, and d_l is the reduced dimension of the coarse surrogate. After determining the dimension of the reduced problem, d_l variables are randomly selected $\{x_{r_1},\ldots,x_{r_{d_l}}\}$, and the database $\boldsymbol{D}$ is reduced to sub - database $\boldsymbol{D}_s$ by extracting d_l variables with index $\{r_1,\ldots,r_{d_l}\}$. Low - fidelity coarse surrogate $\hat{f}_{coa}$ is then constructed using GRNN. The most promising solutions in the sub - database $\boldsymbol{D}_s$ are chosen as the current population $P=\{\mathbf{x}_{s_1},\ldots,\mathbf{x}_{s_i},\ldots,\mathbf{x}_{s_{NP}}\}$, where $\mathbf{x}_{s_i}$ contains the variables with index $\{r_1,\ldots,r_{d_l}\}$. Differential evolutionary operators are then employed to generate offspring $P'=\{\mathbf{u}_{s_1},\ldots,\mathbf{u}_{s_i},\ldots,\mathbf{u}_{s_{NP}}\}$. The most promising individual $\hat{\mathbf{u}}_{s_{best}}$ is prescreened by coarse surrogate $\hat{f}_{coa}$:

$$\hat{\mathbf{u}}_{s_{best}} = \underset{\mathbf{u}_{s_i}\in\{\mathbf{u}_{s_1},\ldots,\mathbf{u}_{s_{NP}}\}}{\arg\min}\ \hat{f}_{coa}(\mathbf{u}_{sub_i}) \tag{17}$$

The corresponding knowledge is further transferred to the fine surrogate search. Detailed procedure for coarse surrogate pre-screening can be found in Algorithm 2.

3.4 Fine surrogate search

High-fidelity fine surrogate $\hat{f}_{fine}$ is constructed using RBF network to predict the landscape of the objective. Nevertheless, more accurate surrogate models may not better guide optimization searches because of the existence of multiple local optima. Approximation errors often benefit the evolutionary search which is known as the effect of 'blessing of uncertainty'. Therefore, knowledge transfer from coarse model to fine model is expected to improve the optimization search by reducing the probability of false convergence into a local optimum. The promising individual $\hat{\mathbf{u}}_{s_{best}}$ provided by coarse surrogate is injected as the transferred point. After transferring the knowledge from the coarse model, the fine model search is then conducted for the remaining variables, which means the original high-dimensional parameter space is reduced into a subspace. DE is employed as the optimizer to locate the optimum for the sub-problem:

$$\hat{\mathbf{x}}_{can} = \underset{\mathbf{x}_{rem}}{\arg\min}\hat{f}_{fine}(\mathbf{u}_{s_{best}},\mathbf{x}_{rem}) \tag{18}$$

where $\hat{\mathbf{x}}_{can}$ denotes the final selected sample point to be evaluated, and $\mathbf{x}_{rem}$ represents the remaining variables except variables with index $\{r_1,\ldots,r_{d_l}\}$. The pseudo-code is described in Algorithm 3, and detailed framework of knowledge transfer between multi - fidelity surrogates and active learning loop for geothermal energy system design and optimization is shown in Fig. 2.

4. Results

In this section, benchmark problems and two real-world geothermal energy system design problems are evaluated to validate the efficacy of the developed algorithm. In the experiments, four CEC benchmark functions are firstly tested in comparison with recently proposed advanced surrogate-guided algorithms, including GPEME, SACOSO, SHPSO and ESAO. To further demonstrate the global optimality of the developed paradigm, two real-world geothermal energy system design problems are further investigated with the aim of maximizing the economic gains of the geothermal system by discovering the optimal well-control scheme. Noteworthy parallel computing can be effectively leveraged during the sampling stage of the DoEs. Besides, distributed sampling can also be conducted by sampling multiple candidate samples. The experiments are conducted in MATLAB R2021a with Intel(R) Xeon(R) Gold 6142 CPU @ 2.59 GHz 64 GB RAM

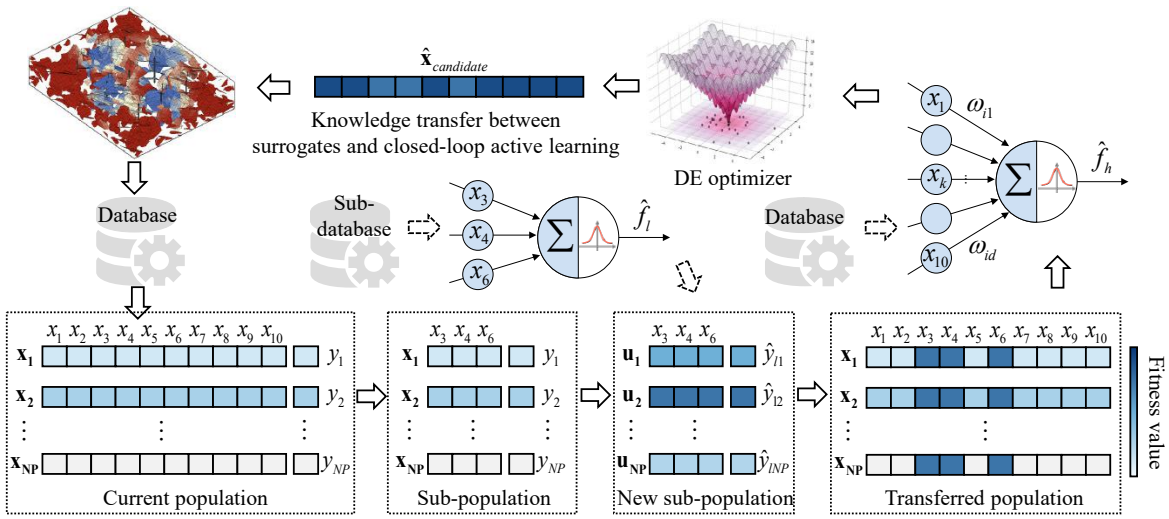

Fig. 2. Framework of multi-fidelity ML surrogates with knowledge transfer and closed-loop active learning for geothermal energy system design and optimization.

Table 1. Characteristics of the benchmarks.

Function	Function expression	Variable range	Properties
Ellipsoid	$\sum_{i=1}^{d} i x_i^2$	$[-5.12, 5.12]^d$	Unimodal
Rosenbrock	$\sum_{i=1}^{d-1} \left[100(x_{i+1} - x_i^2)^2 + (x_i - 1)^2\right]$	$[-2.048, 2.048]^d$	Multimodal
Ackley	$-20\mathrm{e}^{-0.02\sqrt{\frac{1}{d}\sum_{i=1}^{d} x_i^2}} - \mathrm{e}^{\frac{1}{d}\sum_{i=1}^{d}\cos 2\pi x_i} + 20 + \mathrm{e}$	$[-32.768, 32.768]^d$	Multimodal
Griewank	$\sum_{i=1}^{d} \frac{x_i^2}{4000} - \prod \cos\left(\frac{x_i}{\sqrt{i}}\right) + 1$	$[-600, 600]^d$	Multimodal

desktop computer.

4.1 Representative benchmark problems

To evaluate the global optimality of MFSKT, experiments are conducted on CEC benchmark suites in comparison with canonical evolutionary algorithm DE and advanced surrogate-guided algorithms, GPEME (Liu et al., 2013), SA-COSO (Sun et al., 2017), ESAO (Wang et al., 2019), and SHPSO (Yu et al., 2018) respectively. The detailed characteristics of the four 50-dimensional benchmark suites are illustrated in Table 1. The optimum of the benchmarks are 0, and the dimension of four benchmarks are 50. Considering the optimization results of evolutionary algorithms are stochastic, 20 independent runs are conducted for all benchmark functions to achieve fair comparison. The initial sampling number is set to 100 function evaluations, and the stopping limit is 500 function evaluations.

To delve into the role of knowledge transfer in optimization, a variant of MFSKT is introduced for comparison purposes. In this variant, solely high-fidelity surrogate models are leveraged to steer the evolutionary algorithm, devoid of any knowledge transfer between multi-fidelity surrogates during the optimization process. Fig. 3 delineates the landscapes of the benchmark functions and the convergence curves of DE, GPEME, SA-COSO, ESAO, SHPSO, the MFSKT variant, and the proposed MFSKT across the four 50-dimensional benchmark problems. In comparison with high-fidelity surrogate search (i.e., MFSKT variant), multi-fidelity surrogates search with knowledge transfer can achieve better convergence and efficiency, showing the great contribution of knowledge transfer. All surrogate-assisted algorithms outperform DE, owing to the high-quality approximation provided by the ML models, which effectively guide the evolutionary search. Notably, while GPEME exhibits relatively lower convergence compared to other surrogate-assisted methods, it distinguishes itself by utilizing a surrogate model to prescreen promising individuals in the population, rather than sampling directly from the surrogate's optimum. In a comprehensive evaluation, MFSKT proves to deliver markedly superior performance compared to existing algorithms across the 50-dimensional benchmark problems, thus presenting a competitive and pioneering simulation-involved optimization framework.

4.2 Geothermal energy system design

To substantiate the efficacy of the proposed algorithm framework, a real-world application focused on fractured geothermal energy systems is conducted. The detailed DFN

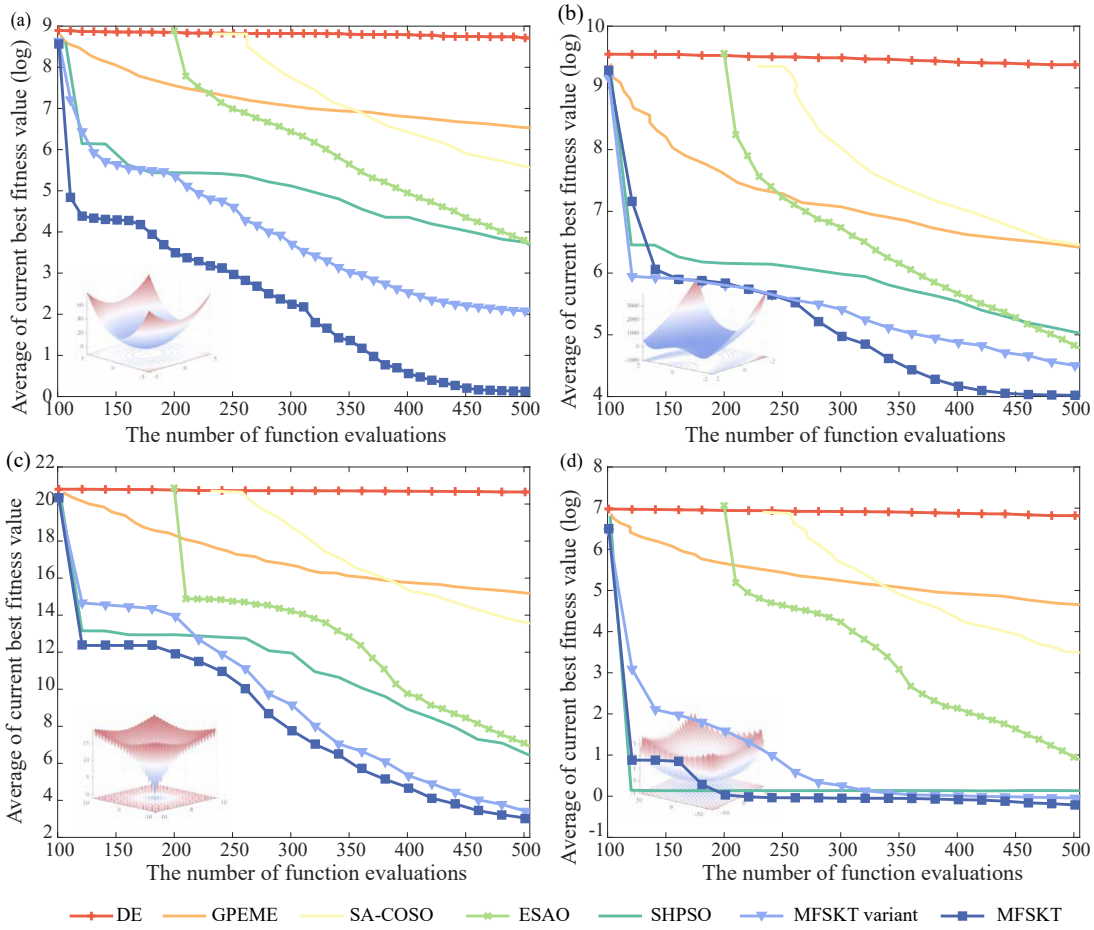

Fig. 3. Benchmark landscapes and optimization result of DE, GPEME, SA-COSO, ESAO, SHPSO, MFSKT variant and the proposed MFSKT on the 50D benchmark problems. (a) Ellipsoid, (b) rosenbrock, (c) ackley and (d) griewank.

model and well location and pattern for the geothermal reservoir is present in Fig. 4. The main goal is to maximize the NPV by ascertaining the optimal well-control schemes for the wells throughout the duration of the project. The model contains two sets of fractures, featuring 4 injectors and five producers. It covers an area measuring $1,000 \times 1,000$ m^2 with 40 m thick. The specific configuration parameters for the fractured geothermal energy system model are enumerated in Table 2. Considering fracture works as the preferential flow, the impact of heterogeneous strata is negligible especially for hot dry rock with limited flow capability. The NPV over the course of the project serves as the target for evaluating the performance. Specifically, the original temperature is 200 °C, while the temperature of injected fluid is 20 °C. The projected lifespan extends to 12,000 days, with each time-step set at 600 days. The producers are maintained at a consistent bottom-hole pressure of 30 MPa. Consequently, the primary objective revolves around ascertaining the optimal fluid injection rates for the 4 injectors across 20 time-steps, a total of 80 parameters to be determined. The ultimate aim is to enhance heat extraction while circumventing uneconomical exploitation throughout the project's duration.

In a comprehensive comparative analysis, canonical DE alongside three advanced surrogate-guided evolutionary computation methods are chosen to validate the performance of the developed method on the fractured geothermal reservoir. Before the active learning process, 100 initial samples are generated uniformly using LHS. Subsequently, 200 iterative active learning sampling is then conducted to iteratively exploit the promising region by surrogate-assisted evolutionary algorithms. Thus, the total number of forward simulation calculations is 300. In light of the stochastic nature of evolutionary algorithms, five independent runs are executed for fair comparison across the five methods.

Fig. 5 presents the averaged convergence curves of various methods (Fig. 5(a)) over 5 independent runs, alongside the corresponding probability density function of the sampled fitness value (Fig. 5(b)) in the active learning process. It emerges from the comparison that the optimization efficiency of DE is quite slow when contrasted with the surrogate-guided evolutionary methods. Notably, GPEME exhibits lower convergence than other surrogate-assisted evolutionary algorithms, attributed to utilizing a surrogate-assisted prescreening strategy, which falls short of the efficiency exhibited by the surrogate-assisted search strategy. SHPSO transcends SOCOSO and GPEME in terms of its optimization capabilities, while the proposed MFSKT not only yields superior efficiency but also excels in optimization effectiveness. Stacked t-SNE visualizations (Fig.

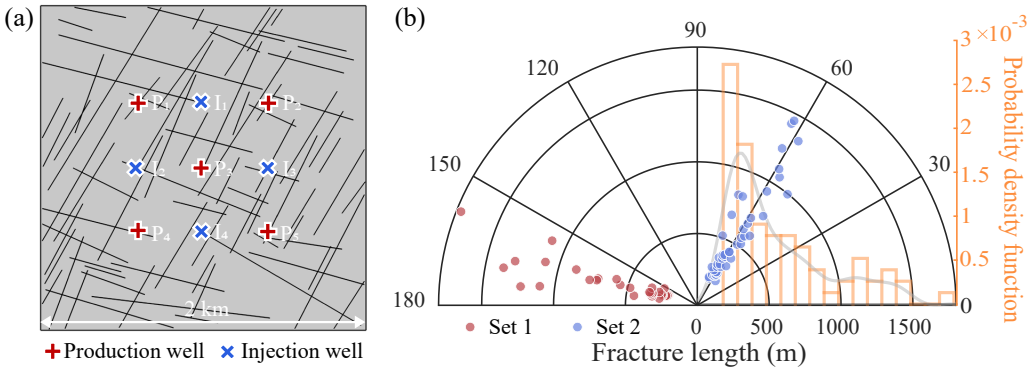

Fig. 4. Discrete fracture network model description for the geothermal energy system. (a) Well-placement and fracture distribution and (b) fracture orientation and length information.

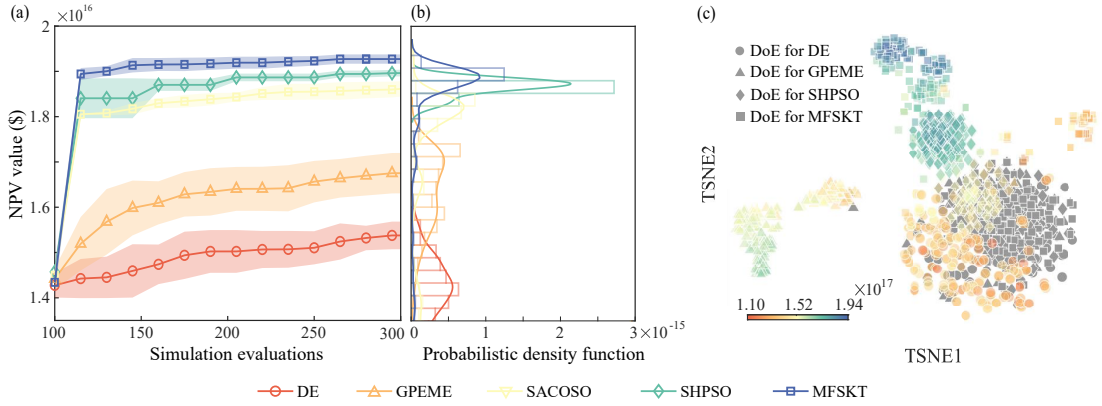

Fig. 5. Optimal design of the fractured geothermal system. (a) Averaged convergence results of canonical DE, advanced surrogate-guided algorithms and the proposed algorithm with 5 independent runs, (b) probability density function of the sampled function value and (c) stacked t-SNE visualizations for the evolutionary history of DE, GPEME, SHPSO and MFSKT.

Table 2. Parameter configurations of the fractured geothermal energy system.

Parameter	Value
Original temperature (°C)	200
Original pressure (MPa)	30
Temperature of injected fluid (°C)	20
Bottom-hole pressure of producers (MPa)	30
Injection rate range of injectors (m^3/s)	$[0, 200] \times 10^{-3}$
Depth (m)	2,500
Matrix porosity (-)	0.01
Fracture porosity (-)	0.1
Matrix permeability (m^2)	5×10^{-17}
Fracture permeability (m^2)	10^{-9}
Formation thickness (m)	40
Matrix heat conductivity (W/(m·K))	2
Fluid heat conductivity (W/(m·°C))	0.698
Matrix thermal capacity (J/(kg·°C))	850
Fluid thermal capacity (J/(kg·°C))	4,200

5(c)) for the evolutionary history of various methods present the sampling history and corresponding fitness distributions. Gray points represent the performance of initially generated solutions by DoE method, while colored points represent the performance of sampled solutions by various methods.

Hydrothermal simulations for the geothermal case are conducted with the optimal well-control schemes of various methods. Temperature distributions with optimal solutions of various evolutionary computation methods of the geothermal case on 3,000, 6,000 and 12,000 days are shown in Fig. 6. Quantitative analysis and comparison for the development performances of the fractured geothermal energy system with the optimized control schemes of various evolutionary methods are illustrated in Fig. 7. The average production temperature of production wells shows a gradual downward trend for all five optimized well-control schemes. As illustrated in Fig. 7(b), the developed MFSKT can achieve a better cumulative NPV after 12,000 days and maintain a relatively high heat extraction rate in the project duration. The optimization scheme for the geothermal energy system provided by MFSKT enhances the profits by maximizing the heat extraction with improved sweep efficiency.

Fig. 8 presents the evolution of cumulative NPV, average temperature of produced fluids and heat extraction rate for the decisions discovered by MFSKT during the optimization

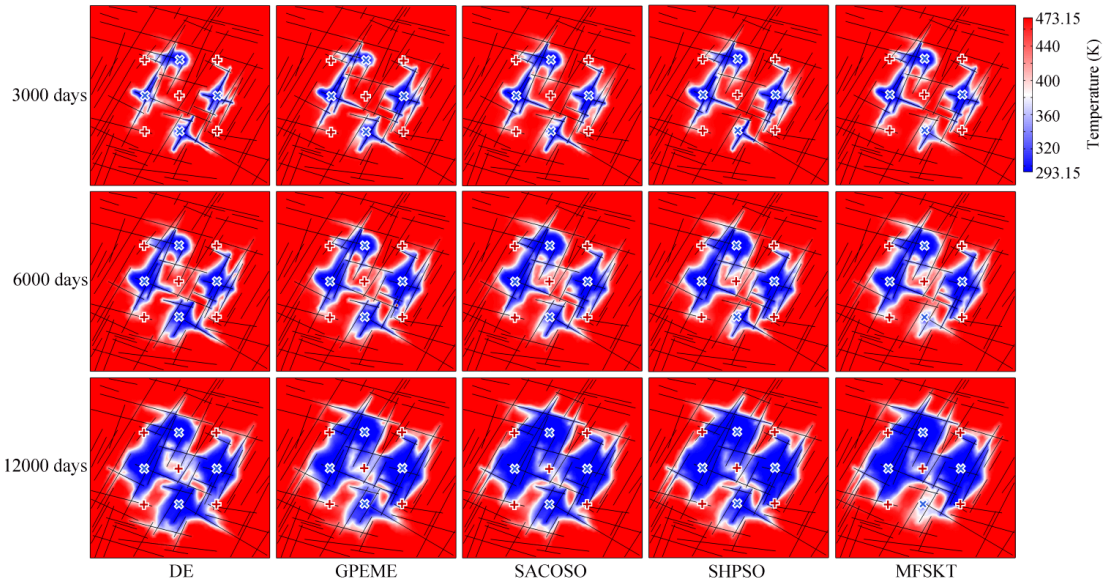

Fig. 6. Temperature distributions with optimal solutions of various evolutionary methods on 3,000, 6,000 and 12,000 days.

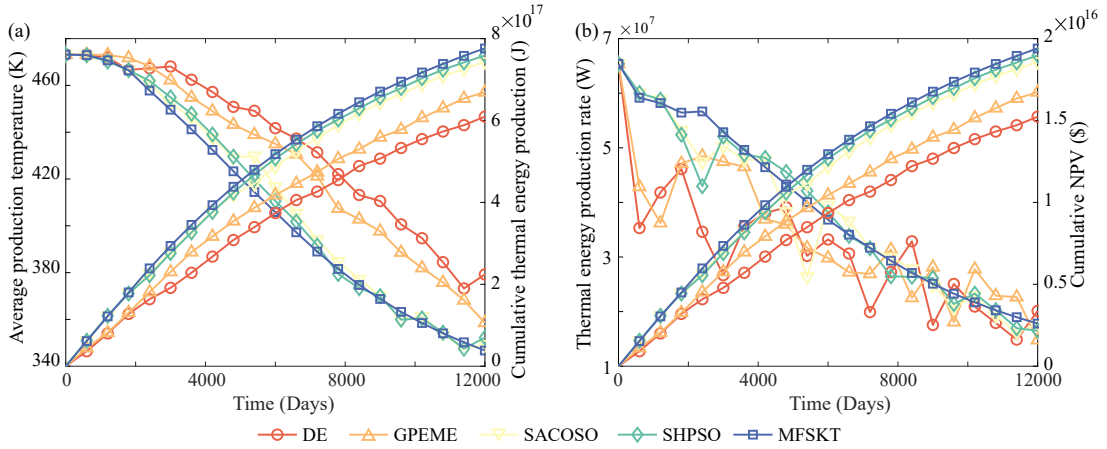

Fig. 7. The development performances of fractured geothermal energy system with the optimized control schemes of various evolutionary methods. (a) Average production temperature versus cumulative thermal energy production and (b) thermal energy production rate versus cumulative NPV.

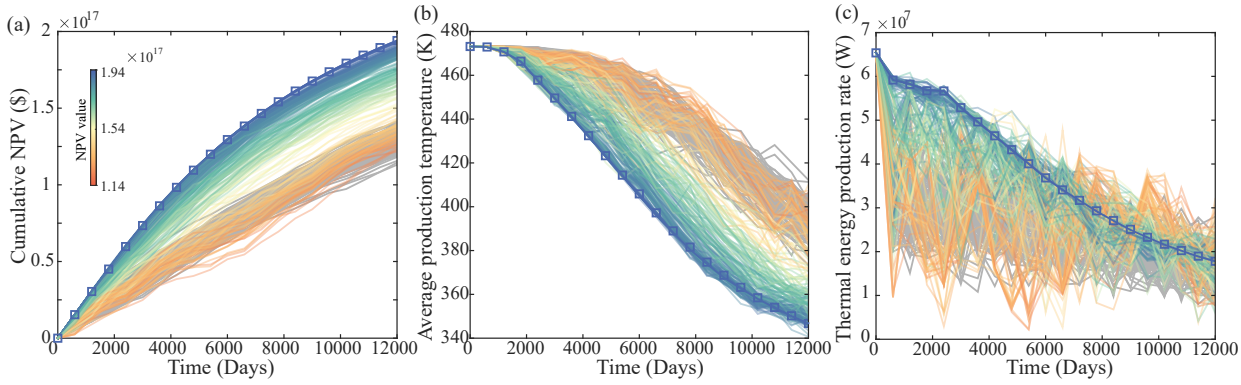

Fig. 8. Evolution of cumulative NPV, average temperature of the produced fluids and heat extraction rate for the decisions discovered by MFSKT method. Evolution history of (a) cumulative NPV for the control schemes discovered by MFSKT method, (b) average temperature of the produced fluids for the decisions discovered by MFSKT method and (c) heat extraction rate for the decisions discovered by MFSKT.

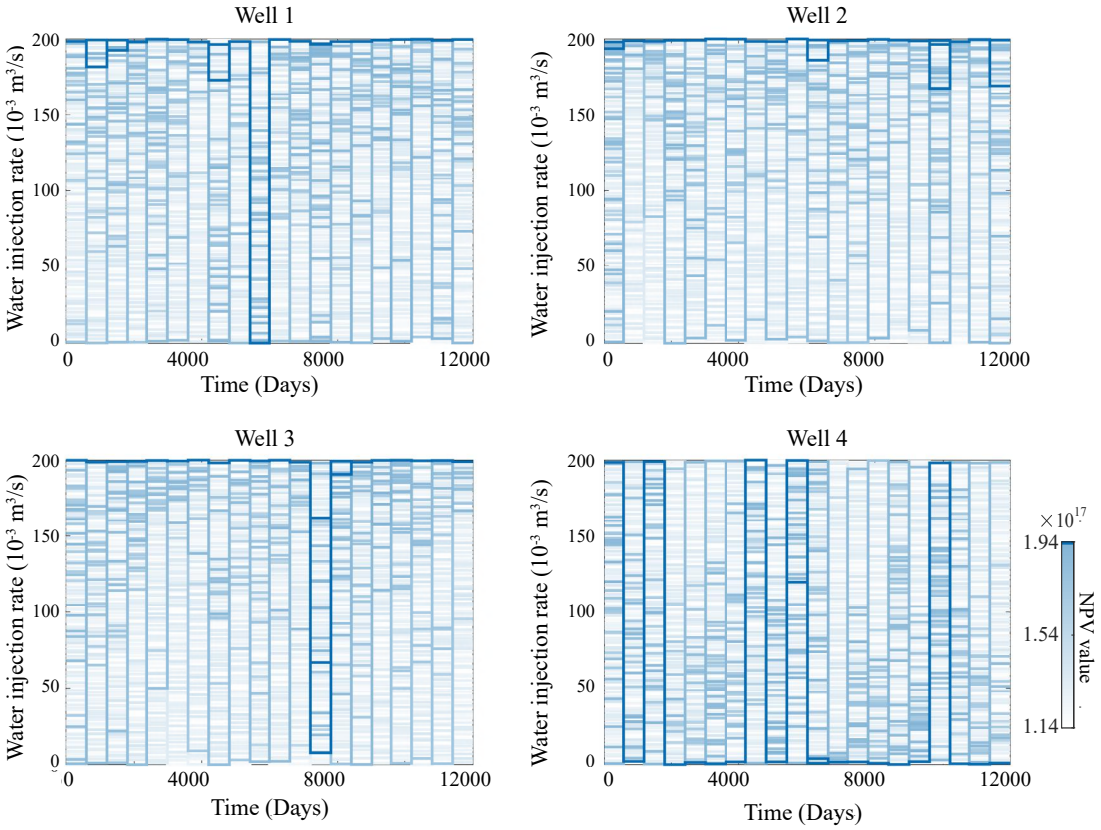

Fig. 9. Evolution for the injection rates for various time-steps of four wells by MFSKT.

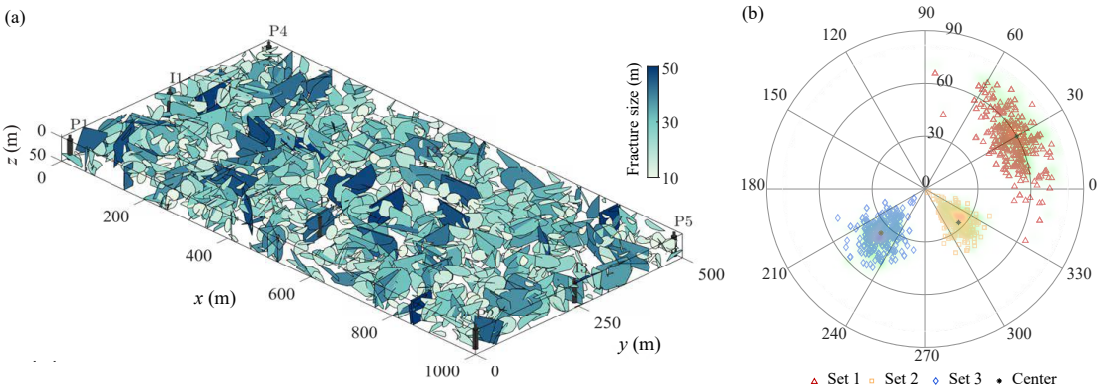

Fig. 10. Large-scale geothermal system containing 1,264 fractures. (a) DFN and well-location configurations of the geothermal system and (b) fracture orientation and length of the DFN model.

process, respectively. The gray lines represent the performance of initially generated well-control schemes, while the colored lines represent the performance of sampled well-control schemes by MFSKT method. The color of the line indicates the NPV value of corresponding well-control scheme. Fig. 9 illustrates the evolution for the well-control schemes of four wells by MFSKT method. Most initially generated well-control schemes by DoE hold relatively low fitness value. After iteratively infill new informative sample points via active learning strategy based on informed acquisition function, surrogate models are updated, and the optimization process is converged efficiently. The method allows for more accurate ML predictions and fewer simulation evaluations, enabling faster convergence by orders of magnitude than canonical evolutionary algorithms.

4.3 Large-scale geothermal system design and optimization

A field-scale geothermal energy system is further employed to compare the optimization efficacy between the proposed method and peer methods. The large-scale EGS comprises more than 1,000 fractures, organized into 3 distinct fracture sets. Elaborate dip direction and distribution of the DFN have been systematically modelled in adherence to the Fisher distribution with $\kappa = 50$, as delineated in Fig. 10 and Table

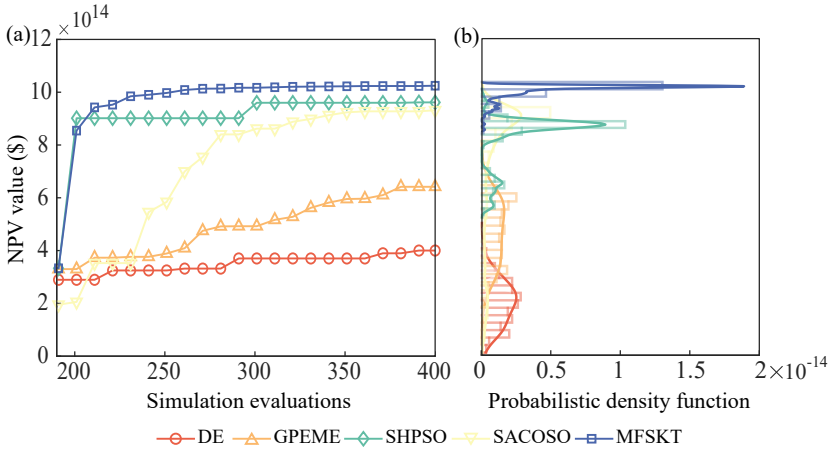

Fig. 11. Convergence curves and probability density function of the sampled objective value in the active learning stage of DE, GPEME, SACOSO, SHPSO and MFSKT for the geothermal system. (a) Averaged convergence results of canonical DE, advanced surrogate-guided algorithms and the proposed algorithm with 5 independent runs and (b) probability density function of the sampled function value.

Table 3. Parameter configurations of the large-scale fractured geothermal energy system.

Parameter	Value
Original temperature (°C)	200
Original pressure (MPa)	30
Temperature of injected fluid (°C)	50
Bottom-hole pressure of injectors (MPa)	$[30, 40]$
Production range of producers (m^3/s)	$[0, 20] \times 10^{-3}$
Depth (m)	3,500
Matrix permeability (m^2)	5×10^{-15}
Fracture permeability (m^2)	10^{-7}
Formation thickness (m)	50
Matrix heat conductivity ($W/(m \cdot K)$)	2
Fluid heat conductivity ($W/(m \cdot K)$)	0.698
Matrix thermal capacity ($J/(kg \cdot K)$)	850
Fluid thermal capacity ($J/(kg \cdot K)$)	4,200

3, detailing the DFN and other parameter configurations of the geothermal energy system. Considering fracture works as the preferential flow, the impact of heterogeneous strata is negligible especially for hot dry rock with limited flow capability. The scale of the model amounts to $1000 \times 500 \times 50$ m^3, encompassing 3 injectors and five producers within the geothermal energy system. The primary goal is the maximization of the NPV accruing from the geothermal reservoir over the course of the project. The NPV is defined as the net thermal extraction value minus the cost associated with fluid production and injection. As the starting point, the large-scale EGS registers a temperature of 200 °C, while the injection water temperature stands at 50 °C. Notably, the projected lifespan spans 6,000 days, with each time-step set at 300 days. The operation of the producers revolves around the fluid production rate, whereas the injectors are governed by the bottom-hole pressure. Hence, the overarching aim of the EGS lies in ascertaining the decision-making for the three injectors and five producers across 20 time-steps, amounting to a total of 160 variables awaiting determination.

This large-scale geothermal energy system is optimized by DE, GPEME, SACOSO, SHPSO and the proposed MFSKT. Due to the high dimensionality of the problem, the initial samples are specified as 200. Afterwards, 200 iterative active learning sampling is then conducted to iteratively exploit the promising region by surrogate-assisted evolutionary algorithms, resulting in a total of 400 forward simulation calculations. Fig. 11 presents the optimization results and probability density function of the sampled objective value in the active learning stage of DE, GPEME, SACOSO, SHPSO and MFSKT for the fractured geothermal energy system. It is observed that DE converges at a slower rate compared to the surrogate-guided evolutionary methods, which leads to unsatisfactory computational performance. Fig. 12 shows temperature distributions with optimal decisions of DE, GPEME, SHPSO and MFSKT for the large-scale DFN model after 1,500, 3,000 and 6,000 days. The injected cold fluid flow into the producers through fractures as the preferential way. It is clear that DE and GPEME achieves more geothermal heat extraction after 6,000 days. Nevertheless, they engaged in excessively uneconomic production after thermal breakthrough, causing low NPV after the project period. SACOSO and SHPSO hold lower thermal sweep efficiency in comparison with MFSKT, resulting in lower NPV after the project period. MFSKT provides a great balance between maximizing geothermal sweep efficiency and reducing redundant and uneconomic development.

The development performances of the fractured geothermal system and associate quantitative analysis with the optimized control schemes of DE, GPEME, SACOSO, SHPSO and MFSKT are shown in Fig. 13. Although the cumulative heat production of MFSKT is not as high as that of DE and GPEME, MFSKT holds the highest cumulative NPV. DE and GPEME excessively and uneconomically exploit geothermal

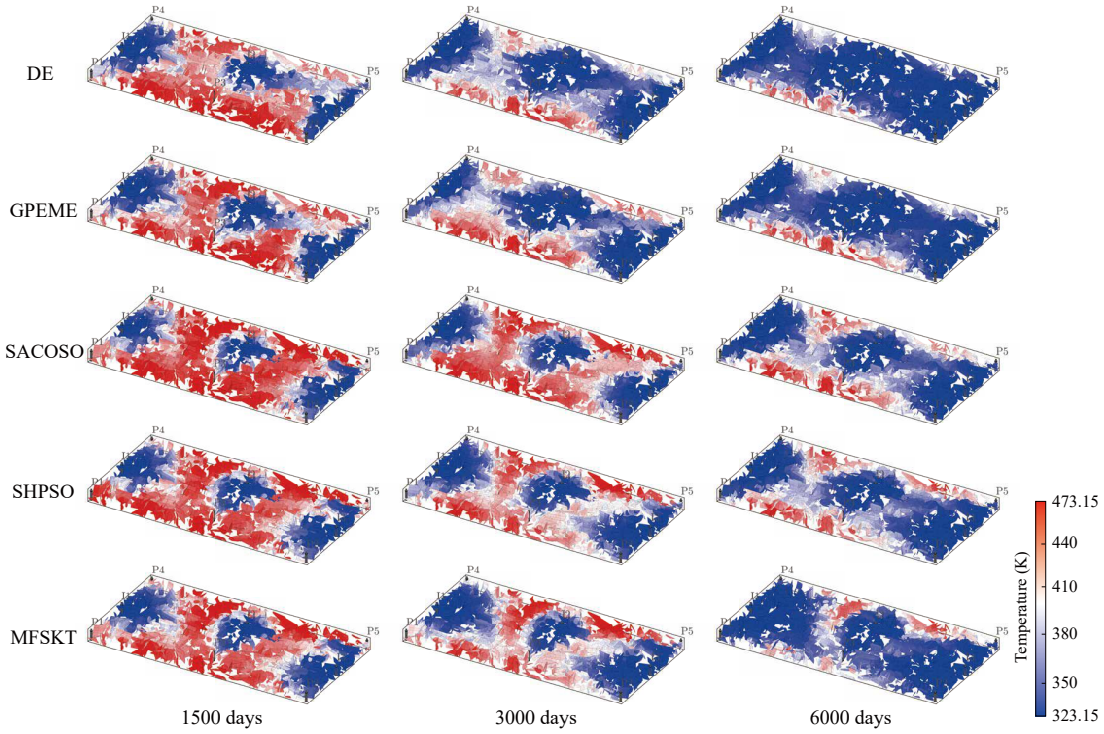

Fig. 12. Temperature distributions with optimal solutions of DE, GPEME, SACOSO, SHPSO and MFSKT for the large-scale DFN model on 1,500, 3,000 and 6,000 days.

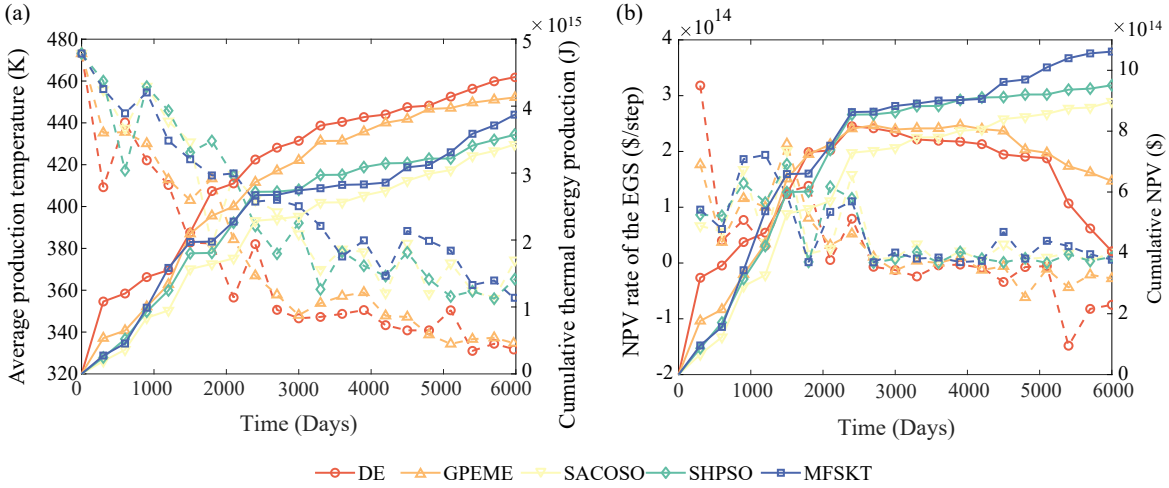

Fig. 13. The exploitation performances of fractured geothermal energy system with optimized control schemes of various evolutionary methods. (a) Average production temperature versus cumulative thermal energy production and (b) thermal energy production rate versus cumulative NPV.

energy after thermal breakthrough, resulting in a downward trend in cumulative NPV in the later stages of the project. The control scheme provided by MFSKT enhances the economic benefits of geothermal system development by delaying geothermal heat breakthrough time, improving heat sweep efficiency, and reducing redundant production. Fig. 14 illustrates the optimized control schemes provided by the algorithms after 400 simulation evaluations. After optimization, the proposed algorithm achieves higher NPV by changing the flow path and displacing the geothermal heat energy in a more economical way.

5. Discussion

A key challenge in geothermal energy production within EGS involves optimizing performance while accounting for the uncertain nature of fracture distribution. Achieving robust control strategies and mitigating development risks hinges on this optimization. The parameters governing the fracture distribution model are subject to uncertainty due to our limited knowledge of subsurface fractured geothermal reservoirs. This, in turn, introduces uncertainty into geothermal prediction. Decision-making under such conditions of uncertain fracture

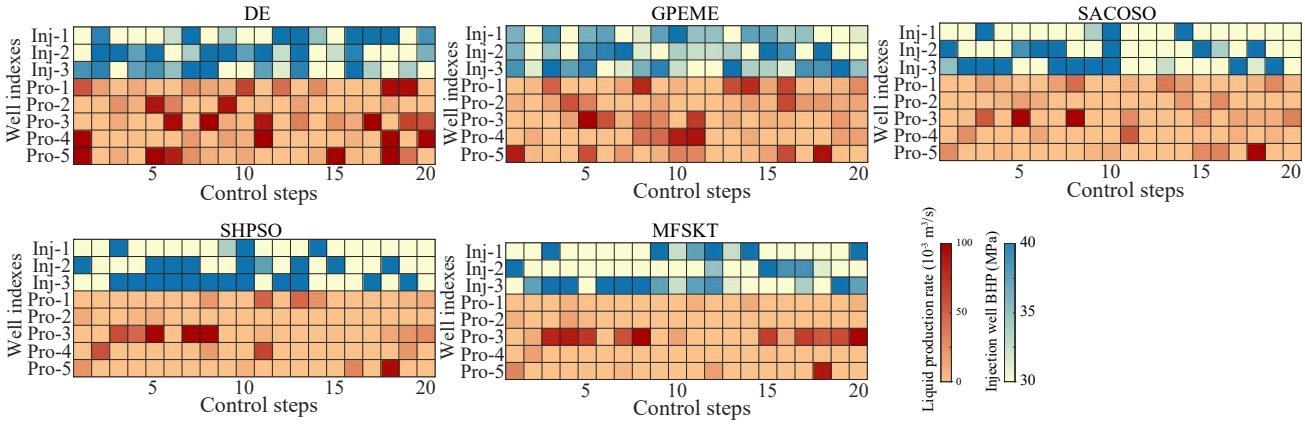

Fig. 14. Final optimal pressure schemes of 8 producers by DE, GPEME, SACOSO, SHPSO and MFSKT for the large-scale geothermal system.

distribution is computationally demanding, as each evaluation of the objective function necessitates multiple simulations. Therefore, further in-depth investigation is required to determine how to leverage surrogate models to decrease the number of computationally expensive simulation calculations and implement optimal design across multiple simulation models to effectively learn the relationships between different fracture network realizations.

Beyond heat extraction challenges, the optimization workflow presented here holds promise for application in a variety of energy systems, particularly those optimization design problems that rely heavily on simulation. The proposed optimization framework offers the potential for efficient and robust optimization across computationally intensive complex systems. How to make full use of the power of generative artificial intelligence for estimation of subsurface fracture network distribution. In future work, generative diffusion models will be used for fracture inference conditioned on observed data to reduce geological uncertainty.

6. Conclusions

In this article, multi-fidelity ML enhanced evolutionary algorithm assisted by knowledge transfer between models is proposed towards heat extraction optimization for fractured geothermal energy systems. The proposed algorithm takes advantage of the data and knowledge by constructing multi-fidelity surrogates, i.e., coarse and fine surrogates, during the optimization process. The coarse model selects some variables randomly to construct a low-fidelity surrogate model, while the fine surrogate uses all variables to construct a high-fidelity surrogate model. Knowledge transfer from coarse surrogate is developed to guide the fine surrogate search into a promising subspace. Active learning is leveraged to refine the accuracy of the ML model by iteratively infusing the most enlightening samples within the parameter space.

Comparative experiments are rigorously performed on benchmark function suites and two real-world EGS in comparison with traditional evolutionary algorithm and advanced surrogate-guided evolutionary methods. After a comprehensive assessment, results demonstrate the efficiency and the effectiveness of the introduced workflow to enhance the real-time decision making of the introduced workflow. Notably, the method substantially diminishes the computational time required for designing geothermal energy systems by multiple orders of magnitude when contrasted with canonical heuristic methods. This work opens doors for accelerated design of fractured EGS and presents promising implications for addressing complex, computationally intensive real-world challenges, including smart grid management, and mechanical metamaterials design.

Acknowledgements

This study is supported by grants from General Fund of Natural Science Foundation of Guangdong Province (No. 2019A151511021), and the HKU Seed Fund for Basic Research.

Conflict of interest

The authors declare no competing interest.

References

Asai, P., Panja, P., McLennan, J., et al. Performance evaluation of enhanced geothermal system (EGS): Surrogate models, sensitivity study and ranking key parameters. Renewable Energy, 2018, 122: 184-195.

Bastek, J. H., Kochmann, D. M. Inverse design of nonlinear mechanical metamaterials via video denoising diffusion models. Nature Machine Intelligence, 2023, 5(12): 1466-1475.

Chen, G., Jiao, J., Jiang, C., et al. Surrogate-assisted level-based learning evolutionary search for geothermal heat extraction optimization. Renewable and Sustainable Energy Reviews, 2024a, 189: 113860.

Chen, G., Jiao, J., Liu, Q., et al. Machine-learning-accelerated multi-objective design of fractured geothermal systems.

Nexus, 2024b, 1(4): 100044.

Chen, G., Luo, X., Jiao, J., et al. Data-driven evolutionary algorithm for oil reservoir well-placement and control optimization. Fuel, 2022, 326: 125125.

Chen, G., Luo, X., Jiao, J., et al. Fracture network characterization with deep generative model based stochastic inversion. Energy, 2023, 273: 127302.

Chen, M., Tompson, A. F. B., Mellors, R. J., et al. An efficient optimization of well placement and control for a geothermal prospect under geological uncertainty. Applied Energy, 2015, 137: 352-363.

Deng, C., Wang, Y., Qin, C., et al. Self-directed online machine learning for topology optimization. Nature Communications, 2022, 13(1): 388.

Ding, P., Zhang, K., Yuan, Z., et al. Multi-objective optimization and exergoeconomic analysis of geothermal-based electricity and cooling system using zeotropic mixtures as the working fluid. Journal of Cleaner Production, 2021, 294: 126237.

Du, X., Damewood, J. K., Lunger, J. R., et al. Machine-learning-accelerated simulations to enable automatic surface reconstruction. Nature Computational Science, 2023, 3(12): 1-11.

Eiben, A. E., Smith, J. J. N. From evolutionary computation to the evolution of things. Nature, 2015, 521(7553): 476-482.

Fan, D., Jodin, G., Consi, T. R., et al. A robotic intelligent towing tank for learning complex fluid-structure dynamics. Science Robotics, 2019, 4(36): eaay5063.

Ghanizadeh, A., Clarkson, C. R., Deglint, H., et al. Unpropped/propped fracture permeability and proppant embedment evaluation: A rigorous core-analysis/imaging methodology. Paper URTEC-2459818 Presented at the SPE/AAPG/SEG Unconventional Resources Technology Conference, San Antonio, Texas, USA, 1-3 August, 2016.

Gupta, A., Ong, Y. S., Feng, L. Multifactorial evolution: Toward evolutionary multitasking. IEEE Transactions on Evolutionary Computation, 2015, 20(3): 343-357.

Gupta, A., Ong, Y. S., Feng, L. Insights on transfer optimization: Because experience is the best teacher. IEEE Transactions on Emerging Topics in Computational Intelligence, 2017, 2(1): 51-64.

Hsieh, P. A., Neuman, S. P., Stiles, G. K., et al. Field determination of the three-dimensional hydraulic conductivity tensor of anisotropic media: 2. Methodology and application to fractured rocks. Water Resources Research, 1985, 21(11): 1667-1676.

Hyman, J. D., Dentz, M., Hagberg, A., et al. Emergence of stable laws for first passage times in three-dimensional random fracture networks. Physical Review Letters, 2019, 123(24): 248501.

Jiang, Z., Ringel, L. M., Bayer, P., et al. Fracture network characterization in reservoirs by joint inversion of microseismicity and thermal breakthrough data: Method development and verification. Water Resources Research, 2023, 59(9): e2022WR034339.

Jin, Y. Knowledge Incorporation in Evolutionary Computation. Luxembourg, Germany, Springer, 2013.

Jin, Y., Wang, H., Chugh, T., et al. Data-driven evolutionary optimization: An overview and case studies. IEEE Transactions on Evolutionary Computation, 2018, 23(3): 442-458.

Jolie, E., Scott, S., Faulds, J., et al. Geological controls on geothermal resources for power generation. Nature Reviews Earth & Environment, 2021, 2(5): 324-339.

Li, B., Wei, Z., Wu, J., et al. Machine learning-enabled globally guaranteed evolutionary computation. Nature Machine Intelligence, 2023a, 5(4): 457-467.

Li, L., Ning, C., Qiu, H., et al. Online data-stream-driven distributionally robust optimal energy management for hydrogen-based multimicrogrids. IEEE Transactions on Industrial Informatics, 2023b, 20(3): 4370-4384.

Li, S., Feng, X., Zhang, D., et al. Coupled thermo-hydro-mechanical analysis of stimulation and production for fractured geothermal reservoirs. Applied Energy, 2019, 247: 40-59.

Liu, B., Zhang, Q., Gielen, G. G. E. A gaussian process surrogate model assisted evolutionary algorithm for medium scale expensive optimization problems. IEEE Transactions on Evolutionary Computation, 2013, 18(2): 180-192.

Liu, Y., Liu, J., Ding, J., et al. A surrogate-assisted differential evolution with knowledge transfer for expensive incremental optimization problems. IEEE Transactions on Evolutionary Computation, 2023, 28(4): 1039-1053.

Menberg, K., Pfister, S., Blum, P., et al. A matter of meters: State of the art in the life cycle assessment of enhanced geothermal systems. Energy & Environmental Science, 2016, 9(9): 2720-2743.

Pan, D., Li, S., Xu, Z., et al. A deterministic-stochastic identification and modelling method of discrete fracture networks using laser scanning: Development and case study. Engineering Geology, 2019, 262: 105310.

Parisio, F., Vilarrasa, V., Wang, W., et al. The risks of long-term re-injection in supercritical geothermal systems. Nature Communications, 2019, 10(1): 4391.

Sanchez-Lengeling, B., Aspuru-Guzik, A. Inverse molecular design using machine learning: Generative models for matter engineering. Science, 2018, 361(6400): 360-365.

Song, G., Song, X., Xu, F., et al. Numerical parametric investigation of thermal extraction from the enhanced geothermal system based on the thermal-hydraulic-chemical coupling model. Journal of Cleaner Production, 2022, 352: 131609.

Specht, D. F. A general regression neural network. IEEE Transactions on neural networks, 1991, 2(6): 568-576.

Sun, C., Jin, Y., Cheng, R., et al. Surrogate-assisted cooperative swarm optimization of high-dimensional expensive problems. IEEE Transactions on Evolutionary Computation, 2017, 21(4): 644-660.

Sun, J., Meng, X., Qiao, J. Data-driven optimal control for municipal solid waste incineration process. IEEE Transactions on Industrial Informatics, 2023, 19(12): 11444-11454.

Wang, C., Liu, J., Wu, K., et al. Solving multitask optimization problems with adaptive knowledge transfer via anomaly

detection. IEEE Transactions on Evolutionary Computation, 2021, 26(2): 304-318.

Wang, J., Zhao, Z., Liu, G., et al. A robust optimization approach of well placement for doublet in heterogeneous geothermal reservoirs using random forest technique and genetic algorithm. Energy, 2022, 254: 124427.

Wang, X., Wang, G. G., Song, B., et al. A novel evolutionary sampling assisted optimization method for high-dimensional expensive problems. IEEE Transactions on Evolutionary Computation, 2019, 23(5): 815-827.

Wang, Z., Zhang, K., Chen, G., et al. Evolutionary-assisted reinforcement learning for reservoir real-time production optimization under uncertainty. Petroleum Science, 2023, 20(1): 261-276.

Wang, Z., Chen, Y., Chen, G., et al. Optimization of geological carbon storage operations with multimodal latent dynamic model and deep reinforcement learning. Geoenergy Science and Engineering, 2025, 244: 213407.

Wen, G., Li, Z., Long, Q., et al. Real-time high-resolution CO_2 geological storage prediction using nested fourier neural operators. Energy & Environmental Science, 2023, 16(4): 1732-1741.

Xu, T., Liang, X., Xia, Y., et al. Performance evaluation of the habanero enhanced geothermal system, australia: Optimization based on tracer and induced micro-seismicity data. Renewable Energy, 2022, 181: 1197-1208.

Xue, X., Chen, G., Zhang, K., et al. A divide-and-conquer optimization paradigm for waterflooding production optimization. Journal of Petroleum Science and Engineering, 2022, 211: 110050.

Xue, X., Yang, C., Hu, Y., et al. Evolutionary sequential transfer optimization for objective-heterogeneous problems. IEEE Transactions on Evolutionary Computation, 2021, 26(6): 1424-1438.

Xue, X., Zhang, K., Tan, K. C., et al. Affine transformation-enhanced multifactorial optimization for heterogeneous problems. IEEE Transactions on Cybernetics, 2020, 52(7): 6217-6231.

Yan, B., Gudala, M., Sun, S. Robust optimization of geothermal recovery based on a generalized thermal decline model and deep learning. Energy Conversion and Management, 2023, 286: 117033.

Yang, C., Ding, J., Jin, Y., et al. Offline data-driven multiobjective optimization: Knowledge transfer between surrogates and generation of final solutions. IEEE Transactions on Evolutionary Computation, 2019, 24(3): 409-423.

Yao, Z., Lum, Y., Johnston, A., et al. Machine learning for a sustainable energy future. Nature Reviews Materials, 2023, 8(3): 202-215.

Yu, H., Tan, Y., Zeng, J., et al. Surrogate-assisted hierarchical particle swarm optimization. Information Sciences, 2018, 454: 59-72.

Zhang, K., Wang, Z., Chen, G., et al. Training effective deep reinforcement learning agents for real-time life-cycle production optimization. Journal of Petroleum Science and Engineering, 2022, 208: 109766.

Zhang, K., Zhao, X., Chen, G., et al. A double-model differential evolution for constrained waterflooding production optimization. Journal of Petroleum Science Engineering, 2021a, 207: 109059.

Zhang, S., Jiang, Z., Zhang, S., et al. Well placement optimization for large-scale geothermal energy exploitation considering nature hydro-thermal processes in the gonghe basin, china. Journal of Cleaner Production, 2021b, 317: 128391.

Zimmerman, R. W., Chen, G., Hadgu, T., et al. A numerical dual-porosity model with semianalytical treatment of fracture/matrix flow. Water Resources Research, 1993, 29(7): 2127-2137.